The Analysis of Thermal Behavior in Ferromagnetic Core Using Boundary Element Method

FÜSUN SERTELLER
Department of Technical Education
Marmara University, Goztepe, Istanbul, 34722
TURKEY
fserteller@marmara.edu.tr

Abstract: **This study presents a method for computing thermal properties of an actuator and compares various magnetic materials. The two-dimensional heat conduction problem is studied using the boundary element method (BEM) with Poisson equivalence. Linear elements are used in the solution procedure. The temperature distribution in the ferromagnetic body is evaluated under stationary condition. The numerical results have been compared with the results of the finite element method (FEM). Numerical experiments have been carried out on soft ferromagnetic materials such as silicon steel iron; mild iron; pure iron and amorf and results the temperature distribution are graphed.**

Key-Words: **Boundary Element Method, ferromagnetic materials, Finite Element Method, thermal analysis, actuator.**

1 Introduction

Computational analyses have been successfully developed using the finite difference (FD), finite element method (FEM) and also the boundary element method (BEM). Recently developed, numerical modeling software has become an indispensable everyday tool for analyzing many kinds of problem (Electrostatics, magnetic field, heat distribution etc.). As the numerical solutions, finite element and finite difference methods give a global solution at any particular point desired. The BEM analysis gives the exact solution at any particular point desired. Also, notice that, although FEM is very commonly used for solving a range of problems, it is time consuming to prepare and modify the finite element discretization, boundary element method (BEM) handles problems with open regions and does not require domain discretization when solving linear problems.

The reported work is focused on the electromagnetic part or in other words on the core; the coil is the heat source within the system. For a standard, electro-thermal core design, the current can be either DC or AC. Multiplication of the supplied voltage and current in the coil per cross section of the core gives the heat source flux (W/m^2) of the ferromagnetic system. For this study 220 V AC- DC contactor core has been used. It has 1630 turns of 0.3 mm diameter. This type of contactor core is suitable for all types of load including transformers, motors and resistive heating loads.

When the electrical energy is applied to the coils, the core starts to heat. The heating temperature differs from one material to another. As the temperature of a ferromagnetic material is increased dramatically its magnetization is decreased and we know modern magnetic materials, with excellent magnetic properties allow to miniaturization of electrical devices and machines. Also in some electrical equipment it can be very useful to calculate the temperature dependent on the currents, especially when high voltages or high currents are studied. For example, when the contacts of contactors or circuit breakers or any kind of these type electrical instruments are submitted high currents, the temperature can increase very quickly and if the contacts of electrical instruments do not open, the conductor can be melt damaging the electromagnetic part. Although the temperature is very important for the application, most of the time, the magnetic circuit temperature is not measured by the manufacturers. For a stable operating condition, temperatures of both core and armature should be kept within expected margins according to operation standards [1, 3,16,32].

2 Thermal effects on Ferromagnetic Material

Ferromagnetic materials are commonly recognized as suitable core materials for high-frequency magnetic devices, such as inductors, transformers actuators and transducers used in modern power electronic systems, because of their attractive characteristics of high permeability, low eddy-current loss, and low cost. Their magnetic properties, on the other hand, are sensitive to the operating temperature.

The temperature in the materials may increase because of energy dissipation which is called the thermal effect. This is not the desired result for ferromagnetic so the temperatures increase should be kept within a limited range in order for the

system to operate effectively. The temperature analyses on materials for different purposes have been widely studied by using 1D or 2D FEM; some examples can be countered as laser surface treatments, to minimize semiconductor devices, etc. The coupled thermal-electric system is of interest in chip-design. [21,22,23].

Strongly magnetic ferromagnetic materials like iron, nickel, cobalt or their combinations even lose all their magnetic properties if they are heated to a high enough temperature. This temperature is called the Curie temperature. The atoms become too excited by the heat to remain pointing in one direction for long. However before reaching this point, magnetic structure begins to fail. The saturation flux density at 100^0 C, for example, can be only about half of that at 20^0 C depending on the type of ferromagnetic materials. A few papers in literature addressed this issue [22,27,32].

From this point of view, ferromagnetic materials are to be said heat sensitive. When the magnetic properties of the materials are increased, the electrical losses or joule heating should be taken into consideration. In addition we should note that, frequency also affects magnetism and temperature. Ferromagnetic materials are used for a variety of uses within the electrical industry including motors, transducers, actuators or galvanometers [15,19].

To prevent any failing under operating condition is necessary to reduce the temperature or the cool side of the equipment that is hottest.

3 Boundary Element Method Program

The Boundary Element method entails the conversion of the partial equation into integral equation, as outlined in [17]. The integrand contains the equivalent source and the free space Green's function or its normal derivative depending on the boundary condition. The usage of the Green function is shown in following section. Boundaries and interfaces are divided into small sections which are referred to as boundary elements.

The accuracy of the approximation will obviously depend upon the choice of the expansion and testing functions, and the number of using them as being other numerical solutions. These coordinate functions must be linearly independent as linear dependence result s in a singular S matrix.

In a typical computer aided design the researcher enters the description of the problem and calculates the parameters of interest. If the values are found to be unsatisfactory, the design is modified and the parameters are recalculated. This process is repeated until satisfactory results are produced. The efficiency of the process is measured by the amount of the time required. The factors that affect the efficiency are the ease of use, the accuracy of the results, the capabilities and the speed of the program.

A numerical technique has been developed using the boundary element method which lends itself very well to open field thermal and electromagnetic problems. The boundary element method approach is gaining recognition within the induction heating industry as being as effective and efficient approach to solving industry specific problems in linear and nonlinear media as well as non homogenous media using boundary only discretization. In addition to boundary only discretization, a distinct feature of BEM is that unknowns which appear in BEM formulation are the surface temperature and heat flux [10,24,28].

Boundary element solutions offer important advantages over domain type methods, such as finite elements and finite difference. The most interesting features of Boundary solutions are the much smaller resulting systems of equations and the considerable reduction, in data required to solve a problem. In addition, the numerical accuracy of boundary methods can be greater than that of the finite element method [18,20].

To implement the method of boundary element, macro flow diagram for both the finite element and boundary element techniques are shown in figure 1. From this comparison, it is obvious that there is one less step involved n BEM compared to completing the same routine using FEM.

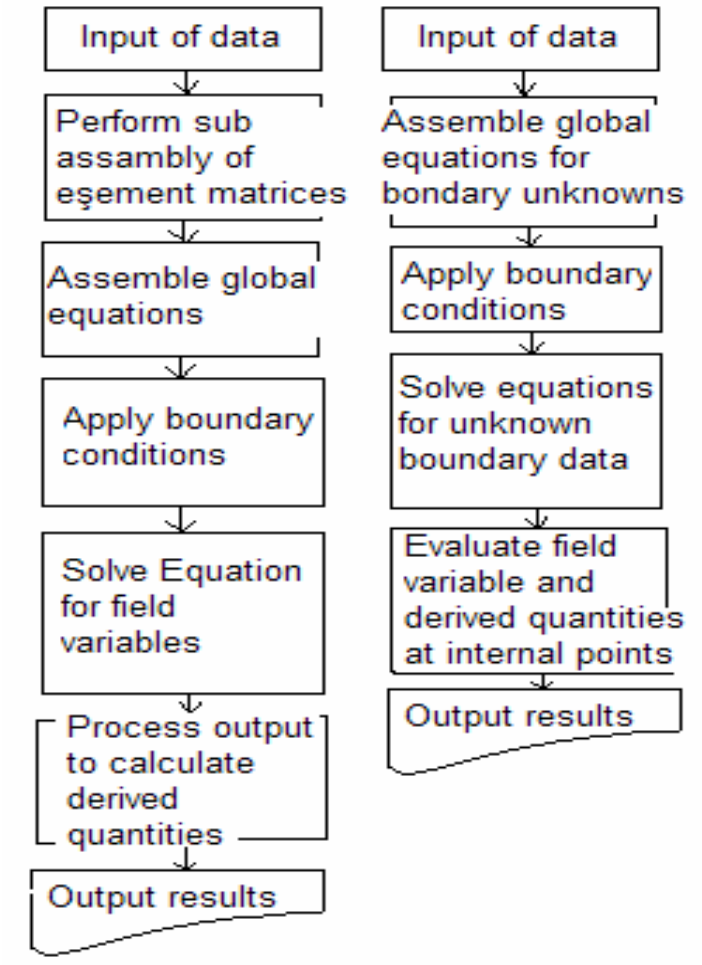

Fig.1 Comparison of flow control in finite elements versus that in boundary elements.
When the two programs are executed simultaneously, it is seen that the distinction in the systems program saves time and unnecessary duplication of effort in the long run. BEM analysis has therefore been preferred for those advantages.

4 BEM Analysis of the Actuator

In this work we considered an actuator whose two dimensional profile is given in Fig. 2. The shaded region consists of coils and the current is transformed into heat to provide a thermal source for the ferromagnetic body. This heat dissipation is called joule losses (Watt) and calculated using the following formula Eq.1:

$$P = I^2 * R \,(\text{Watt}) \tag{1}$$

"I "is the current and (A)" R "is the resistance of the coil (Ω).

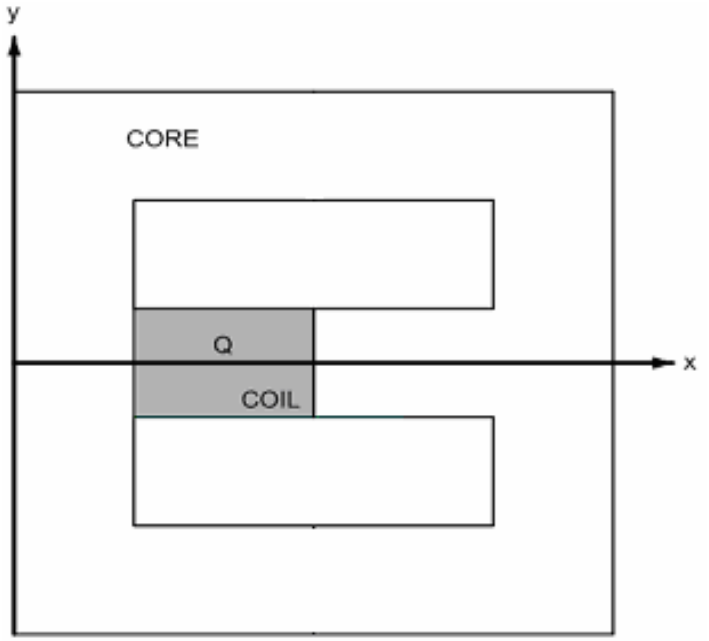

Fig.2. A planar cross-section of the ferromagnetic core

It is now intended to evaluate temperature distribution throughout a planar cross-section of the ferromagnetic core. Since the problem inherits a symmetry with respect to the x-axis, we consider only the part of the device where ($y \geq 0$) part of the device. The formulation of the problem (Eq.(2)) is given such that [4]

$$\frac{\partial^2 T(x,y)}{\partial \mathrm{x}^2} + \frac{\partial^2 T(x,y)}{\partial \mathrm{y}^2} = -\frac{1}{k} Q(x,y) \tag{2}$$

where T is temperature, Q is heat source and k is the thermal conduction coefficient of the actuator metal. Eq. (2) is subject to the boundary conditions

$$\frac{\partial T(x,y)}{\partial \mathrm{y}} = 0 \tag{3a}$$

For $y = 0$ as symmetry condition and

$$\frac{\partial T(\vec{r})}{\partial n} + \frac{h}{k} T(\vec{r}) = \frac{h}{k} T_0 \tag{3b}$$

For the rest of the boundaries including the air gap in the middle for natural convective air cooling, mixed boundary condition was used. In Eq. (3), h and T_0 denote the heat transfer coefficient of air and ambient temperature at normal conditions, respectively.
For the BEM formulation, we define the Green's function as a solution of the equation,

$$\nabla^2 T(\vec{r}) = -\frac{1}{k} Q(\vec{r}) \tag{4a}$$

$$\nabla^2 G(\vec{r}, \vec{\rho}) = -\frac{1}{k} \delta(\vec{r} - \vec{\rho}) \tag{4b}$$

And multiplying equations, it is written following

$$G(\vec{r}, \vec{\rho}) \nabla^2 T(\vec{r}) = -\frac{1}{k} Q(\vec{r}) G(\vec{r}, \vec{\rho}) \tag{5a}$$

$$T(\vec{r}) \nabla^2 G(\vec{r}, \vec{\rho}) = -\frac{1}{k} T(\vec{r}) \delta(\vec{r}, \vec{\rho}) \tag{5b}$$

Subtracting eq. (5a) from eq. (5b)

$$G(\vec{r}, \vec{\rho}) \nabla^2 T(\vec{r}) - T(\vec{r}) \nabla^2 G(\vec{r}, \vec{\rho}) = -\frac{1}{k} Q(\vec{r}) G(\vec{r}, \vec{\rho}) + \frac{1}{k} T(\vec{r}) \delta(\vec{r} - \vec{\rho}) \tag{6a}$$

$$T(\vec{r}) \delta(\vec{r}, \vec{\rho}) = Q(\vec{r}) G(\vec{r}, \vec{\rho}) + k G(\vec{r}, \vec{\rho}) \nabla^2 T(\vec{r}) - k T(\vec{r}) \nabla^2 G(\vec{r}, \vec{\rho}) \tag{6b}$$

where $\vec{r}$ and $\vec{\rho}$ are field and source points, respectively. Substituting Eqs (6) into (2) and integrating over the problem domain V, and using integration by parts, the boundary integral equation form of Eq. (2) can be written in the general form [5-7]

$$T(\vec{\rho})=\int_V d\vec{r}\,Q(\vec{r})G(\vec{r},\vec{\rho})+k\int_\Gamma d\Gamma\left[G(\vec{r},\vec{\rho})\frac{\partial T(\vec{r})}{\partial n}-T(\vec{r})\frac{\partial G(\vec{r},\vec{\rho})}{\partial n}\right] \tag{7}$$

Where *n* is the surface normal and Q is a harmonic function, at boundaries:

$$c(\vec{\rho})T(\vec{\rho})=$$

$$\int_V d\vec{r}(\vec{r})Q(\vec{r})G(\vec{r},\vec{\rho})+k\int_\Gamma d\Gamma\left[G(\vec{r},\vec{\rho})\frac{\partial T(\vec{r})}{\partial n}-T(\vec{r})\frac{\partial G(\vec{r},\rho)}{\partial n}\right] \tag{8}$$

Further we can write equation (8),

$$c(\vec{\rho})T(\vec{\rho})=\int_V d\vec{r}Q(\vec{r})G(\vec{r},\vec{\rho})+k\int_\Gamma d\vec{r}G(\vec{r},\vec{\rho})\frac{\partial T(\vec{r})}{\partial n}$$

$$-k\int_\Gamma d\vec{r}T(\vec{r})\frac{\partial G(\vec{r},\vec{\rho})}{\partial n} \tag{9}$$

So breaking down Γ to $\Gamma=\Gamma_1+\Gamma_2+\Gamma_3$ the equation is written as follows

$$c(\vec{\rho})T(\vec{\rho})=\int_V d\vec{r}Q(\vec{r})G(\vec{r},\vec{\rho})+k\int_{\Gamma_1} d\vec{r}G(\vec{r},\vec{\rho})\frac{\partial T(\vec{r})}{\partial n}$$

$$+k\int_{\Gamma_2} d\vec{r}G(\vec{r},\vec{\rho})\frac{\partial T(\vec{r})}{\partial n}-k\int_{\Gamma_3} d\vec{r}T(\vec{r})\frac{\partial G(\vec{r},\vec{\rho})}{\partial n} \tag{10}$$

Submitting boundary conditions equations (3a) and (3b) into equations (10)

$$c(\vec{\rho})T(\vec{\rho})=\int_V d\vec{r}Q(\vec{r})G(\vec{r},\vec{\rho})+k\left[\frac{h}{k}T_0-\frac{h}{k}T(\vec{r})\right]$$

$$\int_{\Gamma_1} d\vec{r}G(\vec{r},\vec{\rho})-\bar{q}\int_{\Gamma_2} d\vec{r}G(\vec{r},\vec{\rho})-k\bar{T}\int_{\Gamma_3} d\vec{r}\,\frac{\partial G(\vec{r},\vec{\rho})}{\partial n} \tag{11}$$

The volume term starting in Eq. (7) can be transformed into surface integral and we can write that U satisfies [7]

$$\nabla^2 U(\vec{r},\vec{\rho})=-G(\vec{r},\vec{\rho}) \tag{12}$$

Then

$$\int_V d\vec{r}\,Q(\vec{r})G(\vec{r},\vec{\rho})=\int_\Gamma d\Gamma\left[Q(\vec{r})\frac{\partial U(\vec{r},\vec{\rho})}{\partial n}-U(\vec{r},\vec{\rho})\frac{\partial Q(\vec{r})}{\partial n}\right] \tag{13}$$

The Green's function which satisfies Eq. (4) with free boundary conditions in two dimensions is given by

$$G(\vec{r},\vec{\rho})=-\frac{1}{2\pi k}\ln\vec{R} \tag{14}$$

Where $\vec{R}=\vec{r}-\vec{\rho}$. This is referred to as an influence function or as a fundamental solution depending upon its particular physical interpretation.

$$(\vec{\rho})T(\vec{\rho})=\int_V d\vec{r}\,Q(\vec{r})\left[-\frac{\ln R}{2\pi k}\right]+\left[hT_0-h\bar{T}\right]$$

$$\int_{\Gamma_1} d\vec{r}\left[-\frac{\ln R}{2\pi k}\right]-\bar{q}\int_{\Gamma_2} d\vec{r}\left[-\frac{\ln R}{2\pi k}\right]-k\bar{T}\int_{\Gamma_3} d\vec{r}\,\frac{\partial}{\partial n}\left[-\frac{\ln R}{2\pi k}\right] \tag{15a}$$

And rearranging Eq.(13a) we have

$$2\pi k(\vec{\rho})T(\vec{\rho})=-\frac{\bar{Q}}{k}\int_V d\vec{r}\ln R-\left[\frac{h}{k}T_0-\frac{h}{k}\bar{T}\right]$$

$$\int_{\Gamma_1} d\vec{r}\ \ln R+\frac{\bar{q}}{k}\int_{\Gamma_2} d\vec{r}\ \ln R-\bar{T}\int_{\Gamma_3} d\vec{r}\,\frac{\partial}{\partial n}\left[\ln R\right] \tag{15b}$$

The boundary is represented with linear elements. The Cartesian co-ordinates x_i of an arbitrary point of an element defined in terms of nodal co-ordinates x_i^c and shape functions can be calculated from

$$x_i=N^c x_i^c \tag{16}$$

where c is the node number which ranges from 1 to 2, i = 1, 2 and N^c are the shape functions of elements defined. Each solution variable, temperature and flux, can then be represented in terms of the same shape functions as follows

$$T=N^c T^c$$
$$q=N^c q^c \tag{17}$$

where T^c and q^c are the nodal values of temperature and flux, respectively. Substituting the parametric representations of geometry, temperature and flux into Eq. (7), for a region wise constant heat source, the boundary integral equation may then be written in the discretized form as

$$c(\vec{\rho})T_s(\vec{\rho}) = \frac{1}{2\pi}\sum_{m=1}^{M}\frac{q_s^c}{k_s}\int_{\Gamma_m} N^c \ln\left|\vec{R}\right| d\Gamma - \frac{1}{2\pi}\sum_{m=1}^{M} T_s^c \int_{\Gamma_m} N_c \frac{\vec{R}.\vec{n}}{R^2} d\Gamma + \frac{1}{4}\sum_{m=1}^{M}\frac{Q_s^c}{k_s}\int_{\Gamma_m} N_c\left[\vec{R}.\vec{n}\left(2\ln\left|\vec{R}\right| - 1\right)\right] \quad (18)$$

where $c(\vec{\rho})$ takes value between 0 and 1 depending on where $\vec{\rho}$ lies [6]. The discretization procedure is fairly simple. It proceeds by breaking Γ down into distinct segments (Fig.3). Since the most accurate result is achieved fine meshing, the study has been completed with the quickest computation time and affective fine-mesh matrix both inside and outside the boundaries.

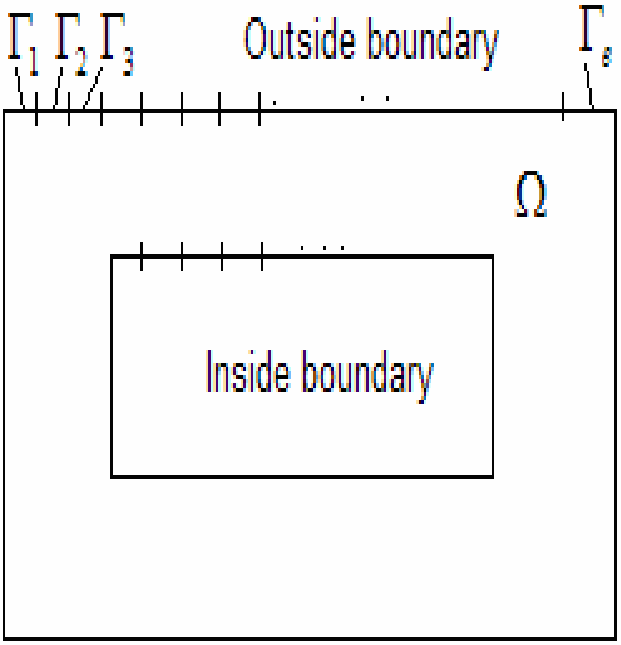

Fig.3 The discretization of the boundary into 'E' elements (each denoted as Γ_e)

The continuous function values are replaced by piecewise continuous function over each element. The unknown function values are sought only the boundary. By discretization only by the boundary, BEM requires a much smaller system of equation. Once the transformation on the boundary is complete, the function values of any internal point can be calculated by an integration involving only function values on the boundary, without having to obtain a solution everywhere. So that, for the problems where the interior and exterior regions are solved simultaneously. The latest research has shown some advantages to using elements with some or all the nodes on the interiors of the elements. These kinds of elements are useful for modeling corners [24,25,31].

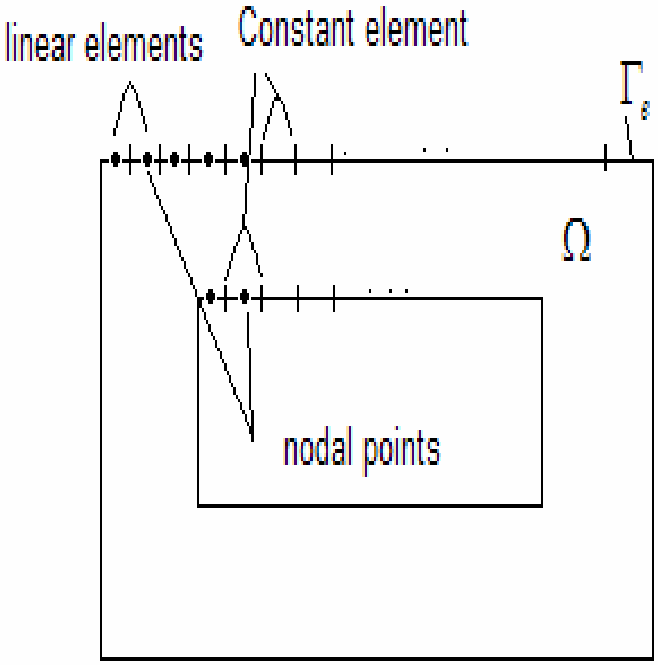

Fig.4 Boundary element discretization into constant and linear elements

In figure 4 linear elements, constant elements and nodal points are highlighted. The discretization on the boundary surface using a patchwork of "elements" is drawn in figure 4 following a specified functional relationship for the desired field variable.

Because of the geometric symmetry of the problem, half of the geometry ($y \geq 0$) has been solved numerically, as shown in fig.2.

Thus in Eq. (18) $c(\vec{\rho})$ is chosen for the multiply-connected domain as follows (see Fig. 1)

$$c(\vec{\rho}) = \begin{cases} 1/4 & \text{corners outside boundary} \\ 3/4 & \text{corners inside boundary} \\ 1/2 & \text{other nodes} \end{cases} \quad (19)$$

Eq. (18) completely defines the solution to the problem when the unknown boundary values are found. We need to first find the values of the derivatives on the boundaries. The accuracy of the BEM essentially depends on the accuracy of evaluation of integrals. Therefore, all integrals in Eq. (18) are calculated analytically. The details of the integration schemes are

covered within the work of previous authors [7, 8, 9,15].

5 Numerical Results

To implement the method, a program was developed using the MATHEMATICA software. In the BEM analysis, 60 and 28 linear boundary elements are considered for the outside and inside boundary, respectively since the boundary element error is reduced by introducing smaller element sizes. The problem domain defines a multiply connected region as shown in Fig. 2.

The linear system constructed according to Eq. (5) is solved by the preconditioned conjugate gradient algorithm [5,26]. The numerical results are tested by the FEM method [6] that based on 204 nodes and 320 triangular elements. Following the boundary solution in the BEM method, internal calculations are performed in the points that they coincide with the FEM nodes. This means that in both methods the temperature is evaluated at the same spatial points.

The BEM results are compared with FEM results along closed contours $K_i = \overline{A_i B_i C_i D_i A_i}$ for $i = 1, 2, 3 \ldots\ldots$ as shown in Fig.5 (contour K). In this study only one contour has been taken but contours are easily expanded as it is required.

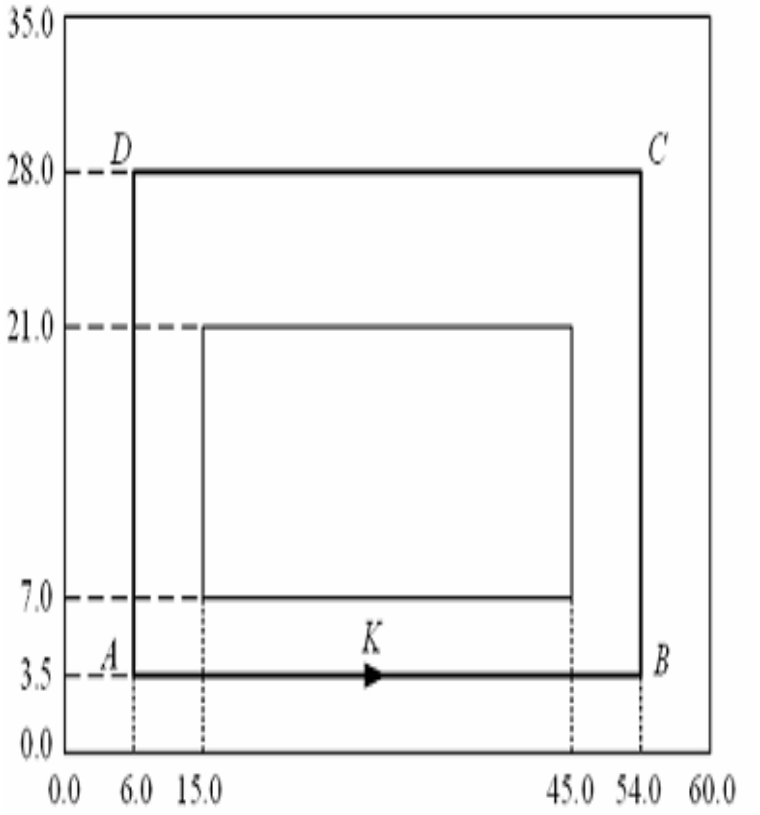

Fig.5. Contour description for temperature variation

In this figure, the contour *K* lies in the centre of the actuator. The test results are given for four materials cast iron, mild steel, silicon sheet iron and amorf in figure 6, 7, 8 and 9 respectively. Clearly visible is that the effect of the electrical losses on the magnetic materials causes various temperature degrees.

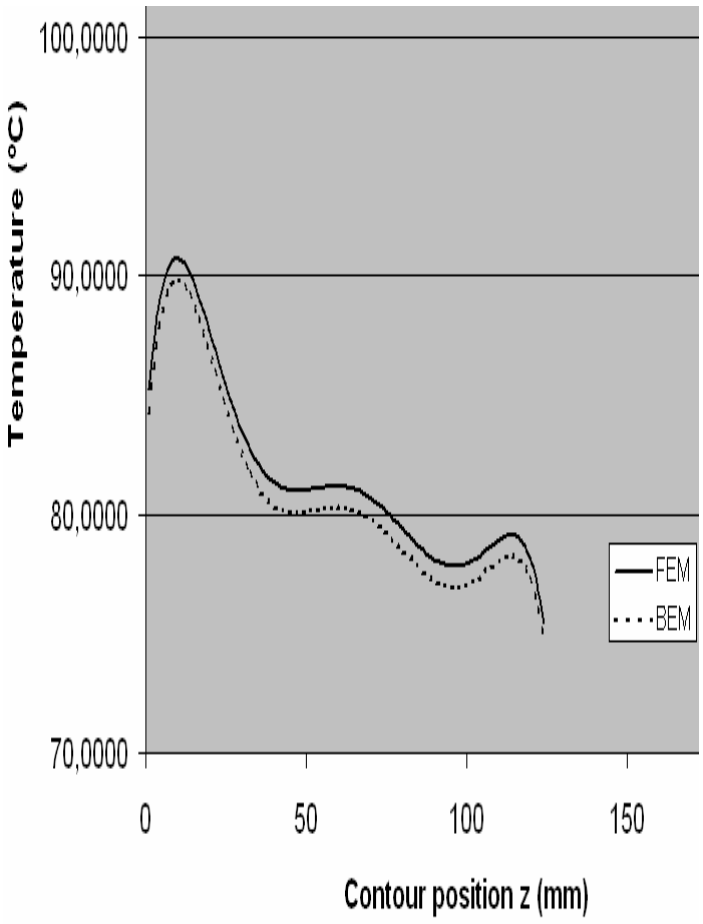

Fig.6. Temperature distributions for cast iron

The cast iron has the lowest magnetic permeability μ value of the four materials. Magnetic permeability is $\mu = 1{,}256 \times 10^{-3}$ H/m ($\mu = \mu_0 \mu_r$, here, μ_0 and μ_r free space and relative magnetic permabilities respectively) at low frequency, like other materials. The peak value of temperature function is between 90^0 C and 95^0 C.

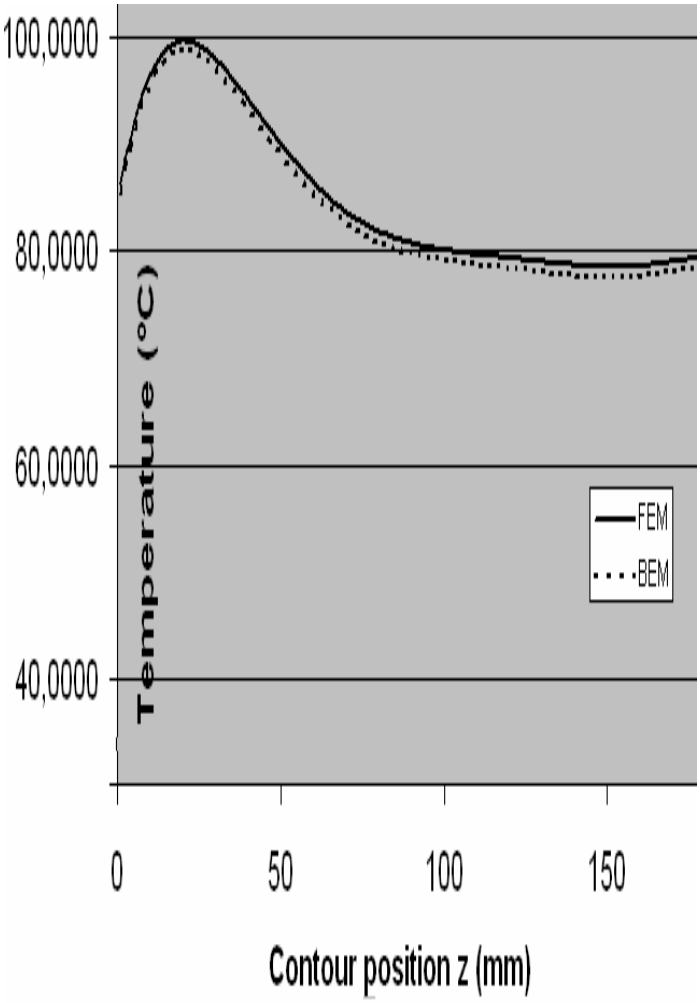

Fig.7.Temperature distributions for mild steel

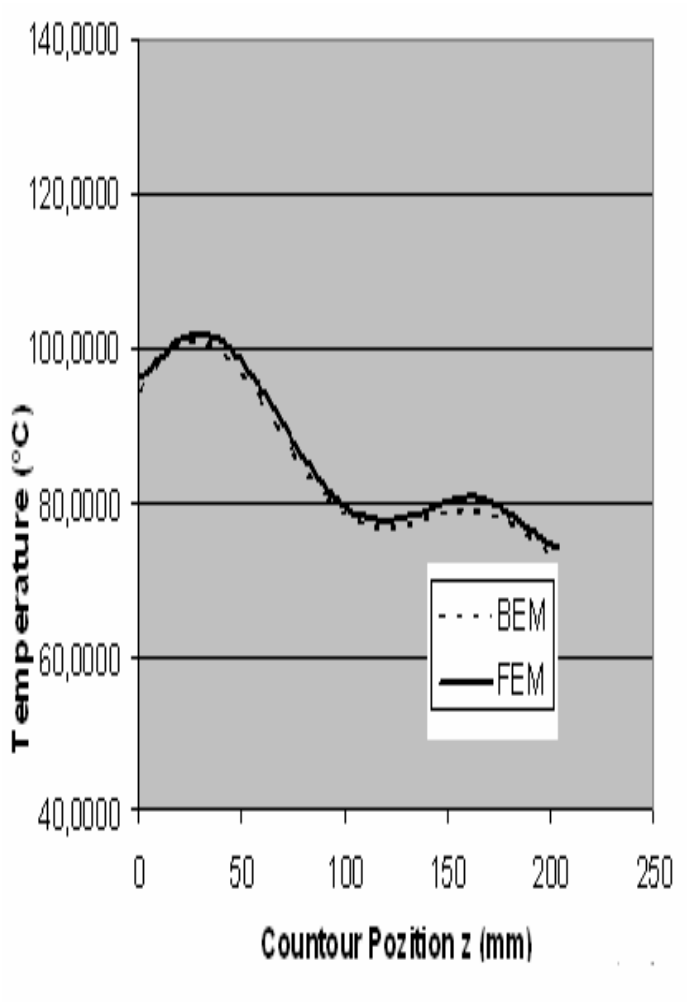

Fig.8. Temperature distributions for silicon sheet iron.

The magnetic permeability of the mild steel is between silicon sheet iron and cast iron, and is taken as $2{,}512 \times 10^{-3}$ H/m for this study (fig.7). The peak temperature is $100\ ^{0}$ C. Mild steel and its compounds are commonly used in the electrical industry, such as in coating technology and the magnetic core of sensor or actuators due to its corrosion protection and electrical insulating respectivly [30,31].

Fig.8 shows temperature distribution for the silicon sheet iron. The peak value of temperature is between 100^{0} C and $105\ ^{0}$ C . Its magnetic permeability is 0, 0892 H/m as high as that of amorf. Silicon sheet iron is commonly used in electromechanical systems such as a core because of it is low cost. To reduce electrical ferrite losses and keep magnetic permeability high, silicon matter is drawn along one side of the each steel slice. It can be considered as an early identified soft magnetic material.

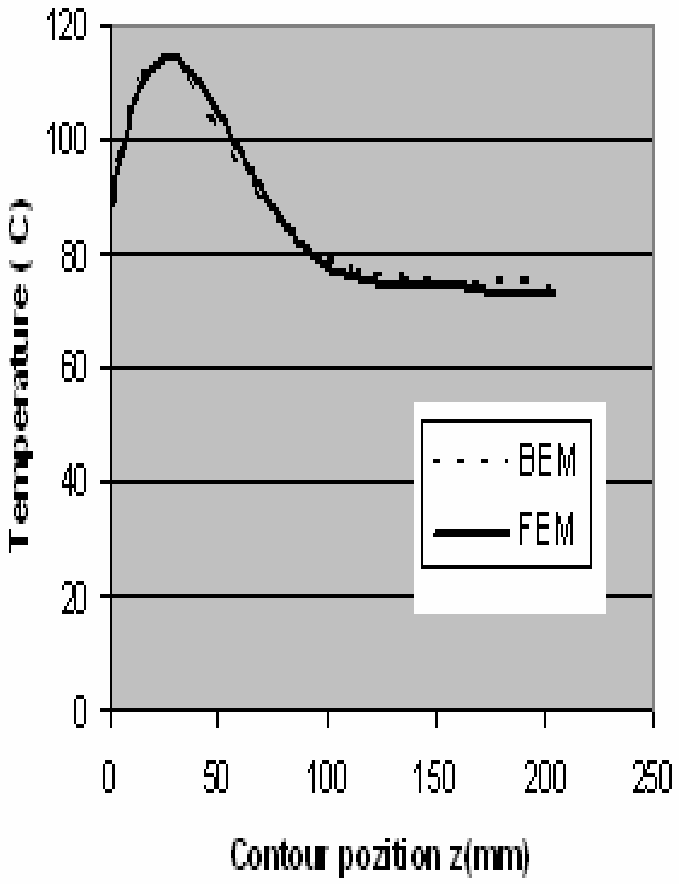

Fig.9. Temperature distributions for amorf

Amorf (Metallic glasses), is manufactured as thin tapes. The Main components of these materials are iron and cobalt. Therefore it would be expected to show similar behaviors as the other ferromagnetic. The temperature peak value is 115 ^{0}C (fig.9). Its magnetic permeability is 0,091 H/m. Previous research has also shown that magnetic susceptibility is not applicable in the high thermal state [29]. Comparisons of the results are given in Figure 10, which shows that the agreement between the results is remarkably good. Figure 10 shows that magnetic permeability and temperature of each specific contactor material are closely interrelated. Figure 10 clearly shows that the lowest heating material is cast iron which has the lowest magnetic permeability. As also seen in the whole figures, solution is not a linear as a function of y, but behaves in a sinusoidal way around the coil region [15, 16, 19,29].

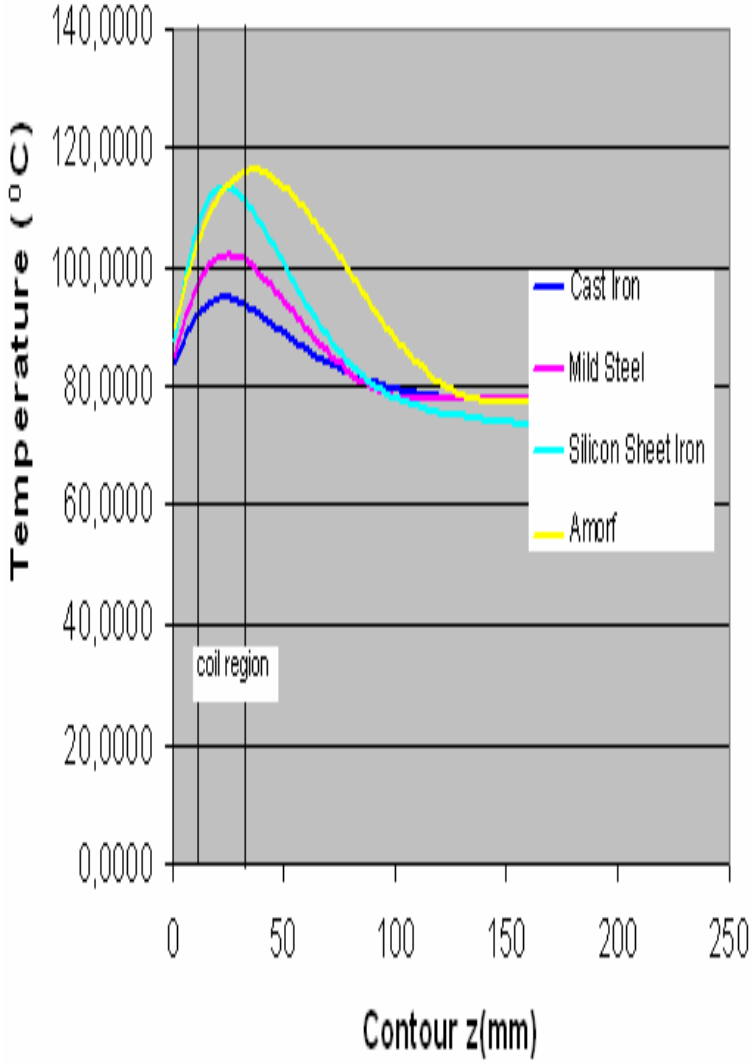

Fig.10. Temperature variation around coils for different core materials

6 Conclusions

In this study, the thermal analysis of actuators cores was investigated. This information would be of use in many operating conditions. Also, the high thermal state of a contactor can affect its magnetic properties. The BEM analysis based on linear elements provides an accurate model for evaluating temperature distribution in the actuator. The BEM results were tested against those using the FEM analysis. Various core materials that are commonly used in electrical devices were simulated. From the comparison of the results (Fig.10) it can be seen that the effect of temperature is more pronounced in amorf than silicon sheet iron, meaning that amorf exhibits a greater temperature rise than other materials. The methodology presented in this paper can be extended to thermal analysis problems of other electrical systems. This is especially relevant for electrical devices with

a ferromagnetic core (i.e. electric motors, transformers, etc.), which are exposed to more severe thermal effects.

Acknowledgment
Author would like to thank Professor Mehmet Akif Atalay for his helpful discussion, review and support during the various stages of this work.

References:

[1] H. Lawrence and V. Vlack, *Elements of Materials Science and Engineering, Reading*, Massachusetts, Addison- Wesley, 1989.

[2] T. Yamada, "An Application of the Dual Reciprocity Boundary Element Method to Magnetic Field and Eddy Current Problems" *IEEE Transaction on Magnetic*, Vol-30, no.5, September 1994.

[3] T.J. Roberts, *The Solution of heat flow equations in large electrical machines*, Pro. IME Vol. 184, PT 3E, pp 70-83,1969-70

[4] A.F. Emiry and W.W. Carson Evaluation of the use of the finite element method in the computation of the temperature, *ASME, Winter Annual meeting*, Nov 16-20, Los Angeles,1969.

[5] A.F. Armor and M.V.K. Chari, Heat Flow in the Stator core of large turbine generators by method of 3-dimensional finite elemens Part I; Analysis by scaler Potential formulation Part II; Temperature Distrubition in the stator iron, *Tran IEEE PAS*, Vol 5, No 5, pp 1648-1668, Sep/Oct, 1976

[6] A. Bousbaine, "Thermal Modeling of Induction Motors based on accurate Loss Density Distribution" *Electric Machines and Power system*, 1999 / 27 / P 311-324.

[7] N. Ozisik, *Heat Conduction*, John Wiley & Sons, (1980).

[8] P. W. Partridge, C. A. Brebbia and L. Wrobel, *The Dual Reciporicity Boundary Element Method*, CMP, Southampton, London, (1992).

[9] A. El-Zafrany, *Techniques of Boundary Element Method*, Ellis Horwood, London, (1993).

[10] G. S. Gipson, *Boundary Element Fundamentals*, CMP, Southampton, (1987).

[11] G. G. Golub and C. F. Van Loan, "Matrix Computations", Baltimore, the Johns Hopkins University Press, 1983.

[12] W.H. Press, S.A. Teukolosky, W.T. Vetterling and B.P. Flannery, Numerical Recipes in FORTRAN Cambridge University Press, Cambridge, 1992.

[13] D. S. Burnett, *Finite Element Analysis*, Reading,Massachusetts, Addison-Wesley, 1987.

[14] S. Nakamura, *Computational Methods in Engineering and Science*, Robert E. Krieger Publishing Company, Florida, 1986.

[15] J.D. Laverns: Numerical solution methods for electro heat problems, *IEEE Transaction on Magnetic*, November, 1983.

[16] L.A. Dobrzonski,M. Drak, B. Ziebowicz, Journal of Achievements in Materials and Manufacturing Engineering, *ASME,* Volume 17, Issue 1-2, July- Agust, 2006.

[17] Y.B. Yildir, "A Boundary Element Method for the Solution of Laplace's Equation in Three-Dimensional Space, *Ph. D. Dissertation*, University of Manitoba, 1985.

[18] R.C. Chen "An iterative Method for Finite Element solution of the non-linear Poisson-Boltzman Equation", *WSEAS transaction on computers*, March 5, 2008.

[19] Y. Shouwen, Z. Liping, Thermal Effect of ferromagnetic materials under cyclic-electric loading, *lecture notes*, Beijing, Chine, 2008.

[20] C.Brebbia,S. Walker, *Boundary Element Techniquesin Engineering*, butterworthes, London, 1980.

[21] Riyad, M. and Abdelkader, H. Comparison between the Analytical and Numerical Methods of solving One-Dimensional Transient Heat Conduction Problems, *Proc. Of the 4th WSEAS Int. Conf. on Heat Transfer, Thermal Engineering and Environment*, Elounda, Greece, 2006, pp 380-384.

[22] J. Mohelnikova, Determination of Specific Heat of a Building Material, *WSEAS Transaction on Heat and Mass Transfer*, Issue 11, Volume 1, November 2006.

[23] A. Bartel, "First order thermal-electric interaction in chip-design", Chair of Applied Mathematics / *Numerical Analysis University of Wuppertal*, bartel@math.uni-wuppertal.de, 2008.

[24] B. Klimpke, C. Rebizant, Two and Three Dimensional Coupled Electromagnetic/Thermal Analysis for Induction Heating Application using the Boundary Element Method, *Integrated Engineering Software*, February 19, 1997.

[25] Z. AndjelicJ. Smajic and M. Conry. Boundary Integral Analysis: Mathematical Aspects and Applications, chapter BEM-based Simulations in Engineering Design. *Springer-Verlag*, 2007.

[26] L. Gaul, M. Kögl and M. Wagner. Boundary Element Methods for Engineers and Scientists. *Springer – Verlag* , Berlin, 2007.

[27] P. L'Eplattenier, G. Cook, C. Ashcraft, M. Burger, A. Shaphiro, G. Daehn, M. Seth, Introduction of E lectromagnetism Module in LS-DYNA for Coupled Mechnanical *Thermal- Electromagnetic Simulations, 9th International LS-DYNA Users Conference,* Dearborn, Michigan, USA, May 30, 2004.

[28] J. Gill, E. Divo, A. Kassab Estimating Thermal Conctact Resistant Using Sensitivity Analysis and Regularization, *Engineering Analysis with Boundary Elements*, online 25 June, 2008.

[29] H.Nishihara,K. Komiyana,I.Ogura, T. Konamato, V.

Chernenko, Magnetization Process near the Curie temperatures of the Itinerant Ferromagnets Ni_2MnCa and Pure Nickel. *Journal of Alloys and Compounds* Volume 442, Issue 1-2, 13 September 2007, Pages 191-193.

[30] F. Canepa, S. Criafici, M. Napoletano,R. Masini, Nonlinear Effects in the AC Magnetic Susceptibility of selected magnetic materials, *Journal of Alloy and Compounds*, 31 July 2006, pages142-145.

[31] G.,G., Gu, M.,A., Gennert, Boundary Element Methods for Solving Passion Equations in Computer Vision Problems, *IEEE Computer Society Conference on Computer Vision,* June 2-6, Hawaii, 1991.

[32] H., Y., Lu, J., G., Zhu, S. Y. R.,Hui, Measurement and Modeling of Thermal Effects onMagnetic Hysteresis of Soft Ferrites, *IEEE Transactıons on magnetıcs*, vol. 43, no. 11, november 2007.